



Emissivity characteristics of polished aluminum alloy surfaces and assessment of multispectral radiation thermometry (MRT) emissivity models

Chang-Da Wen, Issam Mudawar *

*Boiling and Two-phase Flow Laboratory, School of Mechanical Engineering, Purdue University,
1288 Mechanical Engineering Building, West Lafayette, IN 47907, USA*

Received 27 February 2004; received in revised form 2 October 2004
Available online 8 December 2004

Abstract

Emissivity characteristics were measured for several polished aluminum alloy samples over the spectral range of 2.05–4.72 μm and temperatures of 600–800 K. Overall, aluminum alloys buck the general trend of increasing emissivity with increasing temperature for metallic surfaces in the infrared range. Only AL 7150 follows the expected trend, while the emissivity of the other alloys decreases between 600 and 700 K and increases between 700 and 800 K, and the emissivity of commercially pure aluminum (AL 1100) decreases monotonically with increasing temperature. The experimental results are used to assess the accuracy of popular multispectral radiation thermometry (MRT) emissivity models for temperature measurement. It is shown that drastic changes in the shape of emissivity distribution preclude the use of a single function to accurately represent every band of the measured spectrum. Better predictions are achieved using the simplest form of MRT emissivity models and minimum number of wavelengths required by the model. Two relatively simple models are identified for best overall predictions for different alloys and temperatures. Despite the relative success of these two models, this study clearly demonstrates that improvements are required in both instrumentation and emissivity models to achieve acceptable accuracy in the implementation of radiation thermometry in the aluminum industry.

© 2004 Elsevier Ltd. All rights reserved.

Keywords: Emissivity; Surface roughness; Aluminum

1. Introduction

Aluminum is one of the most important metals in modern industry. With its inherent attributes of high strength-to-weight ratio, corrosion resistance, and full

recyclability, aluminum can be found in virtually every type of industry. Examples include aircraft and satellite structures, electronic chasses, window frames, soda cans, and, more recently, automobile frames, engine block, and body panels.

Despite aggressive recycling efforts, aluminum remains far more expensive than steel. This is why efforts to introduce aluminum into applications that rely heavily on steel have been rather slow. With increased competitiveness, there is now a pressing need to produce high quality aluminum parts and reduce production

* Corresponding author. Tel.: +1 765 494 5705; fax: +1 765 494 0539.

E-mail address: mudawar@ecn.purdue.edu (I. Mudawar).

Nomenclature

c_1	first thermal radiation constant
c_2	second thermal radiation constant
DWRT	dual-wavelength radiation thermometry
HRR	Hagen–Rubens emissivity model
IST	inverse spectral temperature emissivity model
IWS	inverse wavelength squared emissivity model
$L_{\lambda,b}$	spectral intensity of blackbody radiation
$L_{\lambda,e}$	spectral intensity of radiation emitted by target surface
$L_{\lambda,gen}$	generated spectral radiation intensity
$L_{\lambda,meas}$	measured spectral radiation intensity
$L_{\lambda,ref}$	spectral intensity of irradiation from surroundings that is reflected by target surface
LEM	linear emissivity model
LLE	log-linear emissivity model
MRT	multispectral radiation thermometry
n	number of unknown coefficients in emissivity model
N	minimum number of wavelengths required in MRT model

R_a	arithmetic average roughness
SRT	spectral radiation thermometry
T	surface temperature
T_{sur}	temperature of surroundings
T_λ	spectral radiance temperature
WLT	wavelength temperature emissivity model

Greek symbols

ε_λ	spectral emissivity
λ	wavelength
ρ_λ	spectral reflectivity

Subscripts

b	blackbody
e	emitted
gen	generated
meas	measured
ref	reflected
sur	surroundings
λ	spectral

cost. A key example of cost-cutting measures is waste reduction by adopting more efficient and better-controlled production methods.

Most processes in aluminum production (e.g., forging, extrusion, rolling) are highly temperature-dependent, and precise determination of the alloy temperature has a strong bearing on both process control and final product quality. During extrusion, for example, accurate temperature measurements are necessary during melting, casting, heating of billets, and profile pressing in order to achieve the desired microstructure and product quality. Many of these processes preclude direct physical contact of a temperature probe with the aluminum surface, especially during profile pressing for parts in transit. These situations require the use of non-contact radiometric means for temperature measurement.

1.1. Radiation thermometry

Radiation thermometry is a convenient non-contact temperature measurement technique that is used to infer surface temperature from the intensity of thermal radiation from the surface, which is referenced to an ideal surface—blackbody—at the same temperature.

The spectral intensity of radiation emitted from a blackbody at temperature T is obtained from the Planck distribution

$$L_{\lambda,b}(\lambda, T) = \frac{c_1}{\lambda^5 (e^{c_2/\lambda T} - 1)}, \quad (1)$$

The intensity of radiation emitted from a real surface is smaller than from a blackbody at the same temperature. Spectral emissivity is the ratio of spectral intensity of radiation emitted by a real surface to that emitted by a blackbody at the same temperature.

$$\varepsilon_\lambda(\lambda, T) = \frac{L_{\lambda,e}(\lambda, T)}{L_{\lambda,b}(\lambda, T)}. \quad (2)$$

A radiation thermometer measures all radiation that is captured at its aperture. This includes, aside from emission from the target surface ($L_{\lambda,e}$), (1) irradiation from the surroundings that is reflected by the target surface, (2) target surface irradiation that is reflected by the surroundings and then the target itself, (3) atmospheric scattering and absorption (H_2O , CO_2 , dust particles, etc.). If the target surface is small compared to the surroundings, the surroundings can be assumed to behave as a blackbody. In this case, the target irradiation reflected by the surroundings and then the target itself can be neglected. In the absence of atmospheric line-of-sight absorption or emission, the measured intensity of an opaque target surface, $L_{\lambda,meas}$, can be simplified as

$$L_{\lambda,meas}(\lambda, T) = \varepsilon_\lambda L_{\lambda,b}(\lambda, T) + \rho_\lambda L_{\lambda,b}(\lambda, T_{sur}), \quad (3)$$

where ρ_λ is the spectral reflectivity of the target surface, which is the fraction of the intensity of irradiation from the surroundings (at T_{sur}) that is reflected by the target surface. For diffuse irradiation from large surroundings, Kirchoff's law shows $\varepsilon_\lambda = \alpha_\lambda$, and for an opaque surface, energy conservation yields $\rho_\lambda = 1 - \alpha_\lambda$.

Substituting these relations into Eq. (3) yields the following expression for the measured radiation intensity of an opaque target surface,

$$L_{\lambda,\text{meas}}(\lambda, T) = \varepsilon_{\lambda} L_{\lambda,\text{b}}(\lambda, T) + (1 - \varepsilon_{\lambda}) L_{\lambda,\text{b}}(\lambda, T_{\text{sur}}). \quad (4)$$

With a known ε_{λ} , the target surface temperature T can be determined from the measured spectral intensity, $L_{\lambda,\text{meas}}$ using Eq. (4). If the target surface is much hotter than the surroundings, the second term on the right-hand-side of Eq. (4) can be neglected without compromising measurement accuracy,

$$L_{\lambda,\text{meas}}(\lambda, T) = \varepsilon_{\lambda} L_{\lambda,\text{b}}(\lambda, T). \quad (5)$$

1.2. Multispectral radiation thermometry (MRT)

Three categories of radiation thermometry are used to determine surface temperature: spectral, dual-wavelength and multispectral. Spectral radiation thermometry (SRT) relies upon intensity measurement at one wavelength and a constant emissivity value to infer the surface temperature. Dual-wavelength radiation thermometry (DWRT) employs intensity measurements at two wavelengths and an emissivity compensation algorithm to determine the surface temperature. Multispectral radiation thermometry (MRT) utilizes intensity measurements at three or more wavelengths and an emissivity model to obtain the surface temperature.

Due to their inability to adequately compensate for the complex emissivity variations of aluminum alloys, SRT and DWRT are only used in a few well-defined situations [1]. The present study will therefore focus entirely on implementation of MRT.

MRT involves observation of spectral radiance at three or more wavelengths and infers the surface temperature by adopting a general model for emissivity behavior. Either (1) empirical functions or (2) analytical functions developed from theoretical premises (e.g., Maxwell, Hagen-Rubens, and Edwards models [2,3]) are used in MRT models. The empirical coefficients in emissivity models provide the MRT method with broad selectivity in representing the complex emissivity variations of aluminum alloys. Moreover, the increased number of wavelengths in MRT (compared to SRT and DWRT) facilitates statistical reduction of temperature error from measurement noise.

Two different mathematical techniques are used in MRT to infer surface temperature. The first method is the *exact technique* which employs radiation intensity measurements at $n + 1$ wavelengths when using an emissivity model with n unknown coefficients. This results in $n + 1$ equations with $n + 1$ unknowns: the target surface temperature, T , and the n unknown coefficients in the emissivity model when applying Eq. (4). Coates [4] and Doloresco [5] concluded the exact technique might cause over-fitting and result in large errors when using more

than three wavelengths. The other method which can overcome the over-fitting problem is the *least-squares* technique. It employs least-squares fitting of measured radiances to simultaneously deduce the values of emissivity coefficients and temperature. This technique is commonly used in MRT and has been studied by many researchers. In this least-squares technique, the number of wavelengths used in the radiance measurements must be at least two greater than the number of unknown coefficients, i.e., spectral intensity measurements should be performed at a minimum of $N = n + 2$ wavelengths.

1.3. Challenges in implementation of MRT method in temperature measurement of aluminum alloys

The complex surface characteristics of aluminum alloys pose serious challenges to the implementation of the MRT method. Low emissivity values of aluminum surfaces produce weak intensity signals. On the other hand, high reflectivity causes large sensitivity to irradiation from the surroundings, which can include several high temperature sources in an actual aluminum production environment. Eq. (4) indicates both of these effects can contribute considerable error in the temperature determination.

Another source of difficulty in implementing the MRT method is the great variety and complexity of aluminum alloy surfaces. The emissivity of aluminum surfaces is influenced by a large number of variables, including alloy composition, temperature, wavelength, surface characteristics (oxidation and roughness), heating time, environment, and process conditions. The profound influence of these effects is evident in Fig. 1, which depicts emissivity variations of AL 2024 with wavelength, temperature, surface roughness and oxidation. These effects remain poorly understood because of both their complexity and the scarcity of reliable published data.

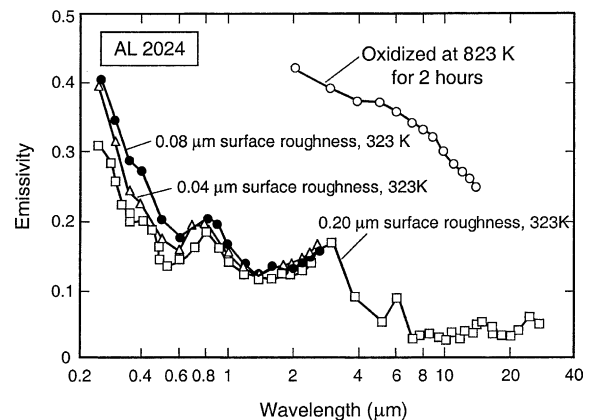


Fig. 1. Spectral emissivity of AL 2024 (adapted from [6]).

Pellerin et al. [7–9] examined several MRT emissivity models for temperature measurement of aluminum alloys. They recommended two empirical models, WLT and IST (these models are discussed in a later section), and a theoretical model, HRR, for wavelengths longer than $1.6\mu\text{m}$. Hopkins [10] examined a second order linear emissivity model (LEM) between 3 and $3.5\mu\text{m}$ for aluminum alloys at 500K. Like Pellerin [7], Hopkins showed LEM produces large errors in the temperature measurement.

The two overriding objectives of the present study are to: (1) conduct a comprehensive experimental study of the effects of temperature, heating time and composition on the spectral emissivity of aluminum alloys, and (2) examine different emissivity models for suitability to predicting the surface temperature of aluminum alloys. Surface intensity is measured for several aluminum alloys and corresponding spectral emissivity calculated. Eighteen MRT emissivity models are examined in pursuit of a model that can improve the accuracy of temperature measurement in the aluminum industry.

2. Experimental methods

2.1. Test facility

As shown in Fig. 2, the experimental apparatus constructed for this study consists of a spectrometer (radiation thermometer), test sample heating assembly, power controller, digital thermometer and data acquisition system. Fig. 3(a) shows the detailed construction of the sample heating assembly. A large aluminum block with an octagonal cross-section is heated by four cartridge heaters which are powered by a variable voltage transformer. The aluminum test sample is pressed against one of the flat surfaces of the heating block

with the aid of an insulating flange made from alumina silicate. All other surfaces of the heating block are covered with a thick blanket of Cotronics high-temperature ceramic fiber insulation. The entire test sample heating assembly is mounted on an X – Y translation platform.

The radiation measurements were made with a Spectraline Model ES100 fast infrared array spectrometer (FIAS). This spectrometer is capable of measuring 160 simultaneous discrete spectral radiation intensity values over a wavelength range of 1.8 – $4.9\mu\text{m}$. Incident radiation at the entrance slit of the FIAS is directed and split into spectral components, and then dispersed over a staggered 160 element linear array PbSe detector. The wavelengths and intensities are found by converting the voltages and pixel numbers recorded on the linear array using pre-installed calibration curves. The intensity data collected in each spectrum is stored at 390Hz. The FIAS output can be either displayed with the aid of a graphical user interface or stored for data analysis.

Fig. 3(b) shows the detailed construction of the test sample and insulating flange. The exposed surface area of the test sample is $15 \times 15\text{mm}^2$. A thermocouple hole is drilled in a vertical plane at a 37° angle to a distance of 1mm from the geometrical center of the exposed surface. The temperature gradient between the exposed bead of a type K thermocouple that is inserted into this hole, and the sample surface is estimated at less than 0.03K, owing to both the high conductivity of aluminum and low heat flux supplied to the sample from the heating block. An Omega 10-channel digital thermometer is used to measure the surface temperature of the sample. The thermocouple measurement was calibrated by an Omega CL1000 hot point dryblock calibrator. The thermocouple readout from the digital thermometer was corrected by the calibration offset,

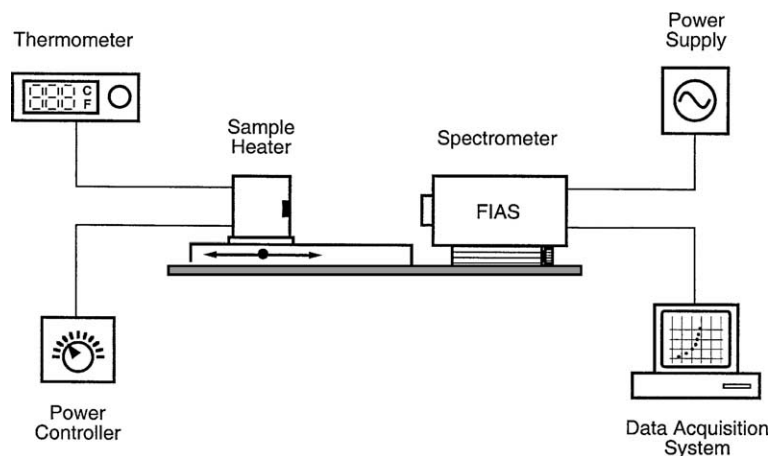


Fig. 2. Temperature measurement facility.

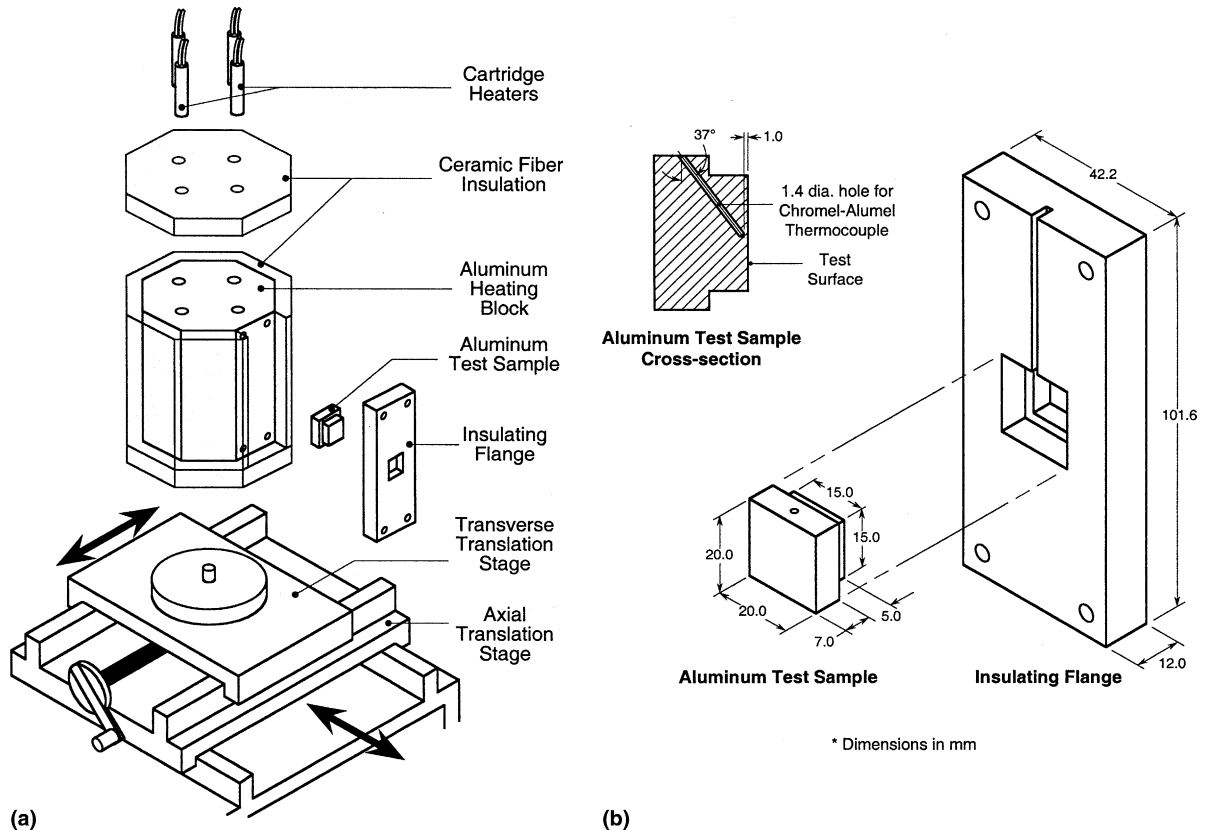


Fig. 3. Construction of (a) sample heating assembly and (b) aluminum test sample and insulating flange.

which was less than 1.6K for a surface temperature of 523K.

2.2. Experimental procedure

Test samples were fabricated from AL 1100 (“commercially pure” aluminum), AL 2024, AL 7075 and AL 7150. The sample surface was polished using a series of five polishing wheels with increasing finer grit and particle size (320 grit SiC, 400 grit SiC, 600 grit SiC, diamond, Gamma alumina); the finishing alumina wheel produced a mechanically mirror polished surface with scratches smaller than $0.05\ \mu\text{m}$. Fig. 4 shows a representative SEM image, a 3D image and a typical surface profile for a polished AL 7075 sample.

After the polishing, each sample was cleaned with acetone then methanol to rid the surface of any oil, grease or dirt. The sample’s thermocouple hole was packed with a thermal conductivity boron nitride powder before the thermocouple was inserted in place.

The heating block was preheated to a temperature slightly above the desired sample temperature. The test sample was pressed against the preheated block with the aid of the insulating flange to initiate heat-up. The

precise sample temperature was achieved by manipulating voltage input to the cartridge heaters. Once the temperature of the sample reached steady-state, the radiance and temperature data were ready to be collected.

The spectrometer was aligned with the test sample using a HeNe laser that was aimed at the center of the sample surface. The sample temperature, measured by the thermocouple, was recorded manually from the digital thermometer and corrected for calibration offset. Three temperatures, 600, 700 and 800 K, were chosen for measurement and analysis. All of the measurements were performed in a controlled laboratory environment with a fairly constant room temperature of 295 K.

3. Results and discussion

The spectral emissivity of individual samples was calculated using Eq. (4), where $L_{\lambda,\text{meas}}$ was measured by the spectrometer, and $L_{\lambda,b}(\lambda, T)$ and $L_{\lambda,b}(\lambda, T_{\text{sur}})$ were calculated from the Planck distribution, Eq. (1), using the sample temperature T measured by the thermocouple, and the room temperature T_{sur} , respectively. The following is a discussion of the effects of sample temperature,

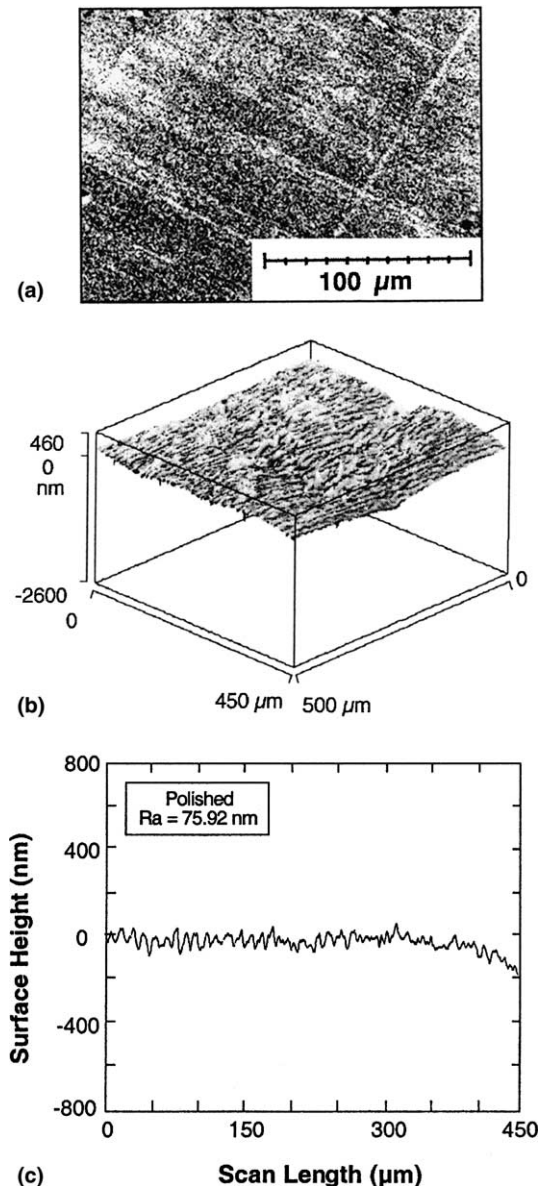


Fig. 4. Surface characteristics of polished AL 7075 sample: (a) SEM image, (b) 3D image, and (c) surface profile.

heating time, and alloy composition on spectral emissivity.

3.1. Effects of temperature

Fig. 5 shows the spectral emissivity distribution for AL 7150 and AL 7075 samples with polished surfaces at 600, 700 and 800 K and wavelengths from 2 to 4.72 μm . Two bands are identified that represent regions of appreciable atmospheric absorption and scattering. The first band is centered around 2.7 μm and is due to room humidity and carbon dioxide; the second is cen-

tered around 4.3 μm and is due to carbon dioxide. Data within the two bands were excluded from the present assessment of emissivity models. It is interesting to note that the emissivity of metallic surfaces in the infrared range typically decreases with increasing wavelength and decreasing temperature [11]. Fig. 5 shows the spectral emissivity for the two aluminum samples do not follow this trend, and the overall shape of the emissivity spectrum changes appreciably with temperature. At 600 K, the emissivity decreases with increasing wavelength for $\lambda < 3.5 \mu\text{m}$, but the trend is reversed at higher wavelengths. Increasing the temperature from 600 to 800 K does not yield the expected increase in emissivity.

Fig. 6 provides an alternative representation of the temperature effects. Here the emissivity at a single wavelength of 3.5 μm is plotted against temperature for each of the four alloys. Only AL 7150 shows a monotonic increase of emissivity with increasing temperature. AL 1100 (commercially pure aluminum) shows the opposite trend, while the emissivity of the two remaining alloys decreases between 600 and 700 K and then increases between 700 and 800 K. The increased emissivity between 700 and 800 K was closely associated with an observed discoloration of the surface from light gray to black, which is common to magnesium-containing alloys [6]. This discoloration was observed on all samples at 800 K except pure aluminum.

3.2. Effects of heating time

Surface oxidation is known to increase the emissivity of a metallic surface that is maintained at an elevated temperature over a period of time. As shown in Fig. 7, the effect of the thermal history on the spectral emissivity of all present aluminum samples shows a measurable increase due to oxidation only during the initial three hours. Thereafter, emissivity remains constant over the next seven hours. This trend is consistent with the findings of previous researchers [8,9]. The present findings suggest future research efforts be focused on relating the rate of increase in emissivity to the alloy-dependant surface oxidation rate only during this initial period.

It is important to note that the data used in the assessment of MRT models in this study, as well as Figs. 5 and 6, were obtained immediately after the sample reached the desired temperature to preclude the aforementioned oxidation effects.

3.3. Effects of alloy composition

Fig. 8 shows the spectral emissivity distribution for the different samples at 700 K. While all alloy samples show similar trends, the pure aluminum sample follows a distinct behavior, with a fairly high emissivity around 2 μm which decreases to the emissivity levels of the alloy samples above 3.5 μm .

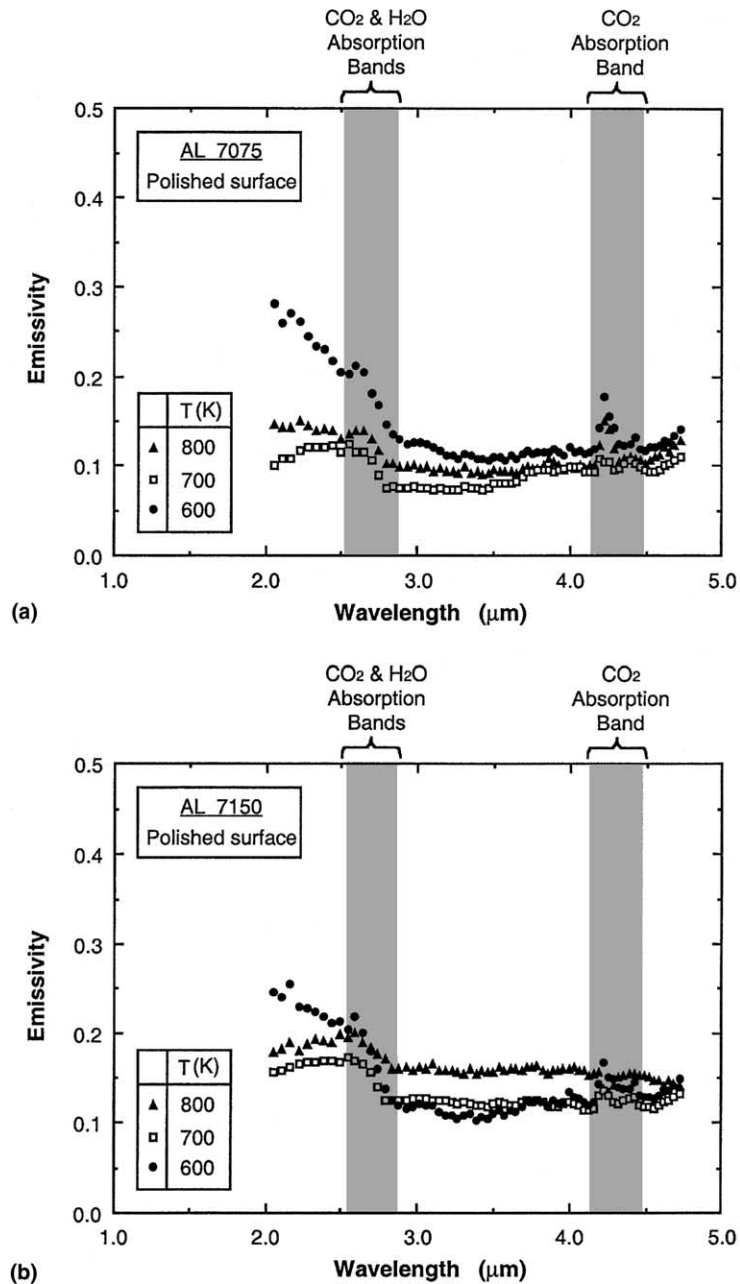


Fig. 5. Effects of temperature on spectral emissivity for (a) AL 7075 and (b) AL 7150.

4. Assessment of MRT emissivity models

Table 1 lists 18 emissivity models that include both mathematical functions (e.g., LLE and LEM) and analytical functions (e.g., HRR) that are examined in the present study for accuracy in temperature determination. They consist of 10 distinct emissivity models and variations to these models based on the number of un-

known coefficients used. The primary goal here is to identify the model(s) that can adequately account for the aforementioned complex variations of emissivity with temperature, wavelength, and alloy composition.

A least-squares fit to the measured radiances is used to simultaneously determine both the unknown coefficients in the emissivity model and the surface temperature. This technique is non-linear and requires

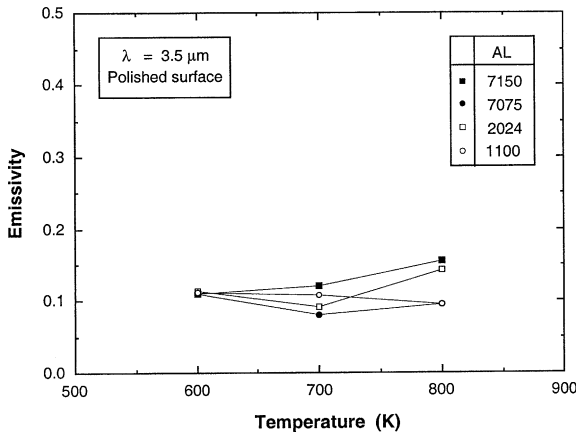


Fig. 6. Effects of temperature on spectral emissivity at 3.5 μm.

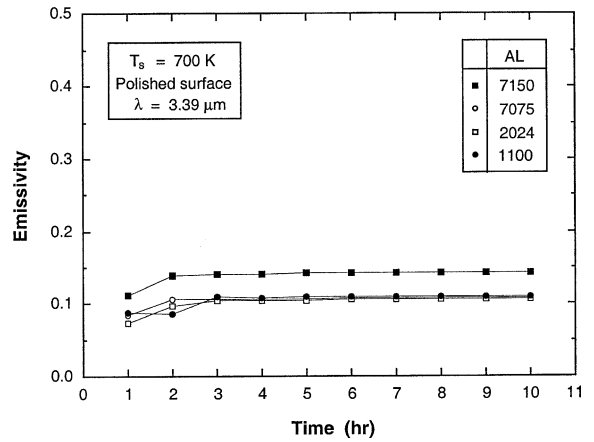


Fig. 7. Effects of heating time on spectral emissivity.

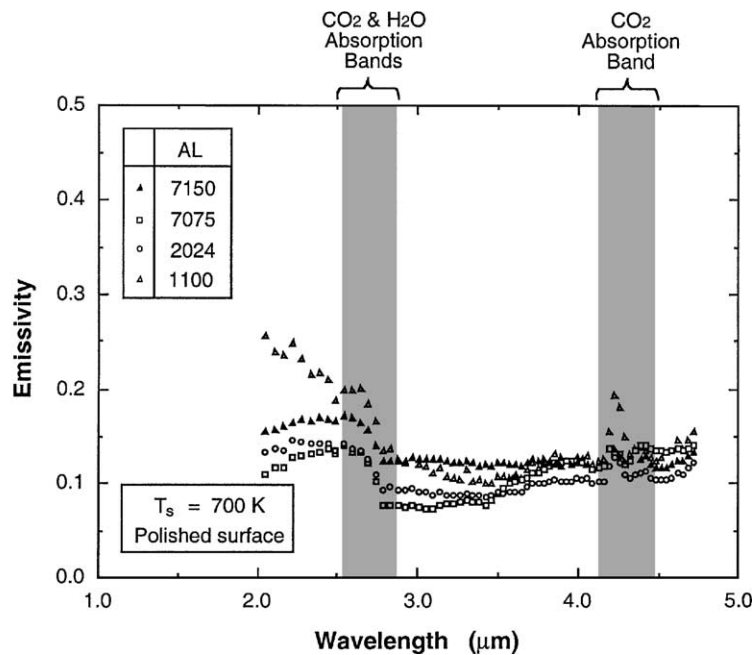


Fig. 8. Effects of alloy on spectral emissivity at 700 K.

numerical iteration. The number of spectral radiance values used in this technique is limited to two more than the number of unknown coefficients in the emissivity model. The inferred temperature and unknown emissivity coefficients are determined by minimizing

$$\sum_{i=0}^n (L_{\lambda, \text{meas}, i} - L_{\lambda, \text{gen}, i})^2,$$

where $L_{\lambda, \text{meas}, i}$ and $L_{\lambda, \text{gen}, i}$ are the measured and generated values of spectral intensity, respectively. Neglecting the intensity of irradiation from the surroundings that is reflected by the target surface and applying Planck

blackbody distribution, Eq. (5) yields the following relation for the generated spectral intensity,

$$L_{\lambda, \text{gen}}(\lambda, T) = \varepsilon_{\lambda}(\lambda) \frac{c_1}{\lambda^5 (e^{c_2/\lambda T} - 1)}. \quad (6)$$

For emissivity models with exponential form, the linear least-squares technique can be used to determine the inferred temperature and unknown emissivity coefficients by minimizing

$$\sum_{i=0}^n (\ln L_{\lambda, \text{meas}, i} - \ln L_{\lambda, \text{gen}, i})^2, \quad (7)$$

Table 1
Mathematical form of emissivity models examined in this study

Emissivity model	Mathematical function
1-1 ^a	$\varepsilon_\lambda = \exp(a_0 + a_1\lambda)$
1-2 ^a	$\varepsilon_\lambda = \exp(a_0 + a_1\lambda + a_2\lambda^2)$
1-3 ^a	$\varepsilon_\lambda = \exp(a_0 + a_1\lambda + a_2\lambda^2 + a_3\lambda^3)$
2-1 ^b	$\varepsilon_\lambda = a_0 + a_1\lambda$
2-2 ^b	$\varepsilon_\lambda = a_0 + a_1\lambda + a_2\lambda^2$
2-3 ^b	$\varepsilon_\lambda = a_0 + a_1\lambda + a_2\lambda^2 + a_3\lambda^3$
3 ^c	$\varepsilon_\lambda = 1/(1 + a_0\lambda^2)$
4 ^d	$\varepsilon_\lambda = a_0(T/\lambda)^{1/2}$
5 ^e	$\varepsilon_\lambda = \exp(a_0\lambda + a_1T)$
6 ^e	$\varepsilon_\lambda = \exp(a_0\lambda + a_1/T_\lambda)^*$
7-1	$\varepsilon_\lambda = \exp(a_0T_\lambda)^*$
7-2	$\varepsilon_\lambda = \exp(a_0 + a_1T_\lambda)^*$
8-1 ^f	$\varepsilon_\lambda = \exp(a_0/T_\lambda)^*$
8-2 ^f	$\varepsilon_\lambda = \exp(a_0 + a_1/T_\lambda)^*$
9-1	$\varepsilon_\lambda = \exp(a_0\sqrt{\lambda})$
9-2	$\varepsilon_\lambda = \exp(a_0 + a_1\sqrt{\lambda})$
10-1	$\varepsilon_\lambda = \exp(a_0/\sqrt{\lambda})$
10-2	$\varepsilon_\lambda = \exp(a_0 + a_1/\sqrt{\lambda})$

* T_λ is spectral radiance temperature defined as equivalent blackbody temperature of measured spectral intensity.

^a Log-linear emissivity model (LLE).

^b Linear emissivity model (LEM).

^c Inverse wavelength squared emissivity model (IWS).

^d Hagen–Rubens model (HRR).

^e Wavelength temperature emissivity model (WLT).

^f Inverse spectral temperature emissivity model (IST).

and by approximating the Planck blackbody distribution used in Eq. (6) by Wien's formula to determinate $L_{\lambda, \text{gen}, i}$

$$L_{\lambda, \text{gen}}(\lambda, T) = \varepsilon_\lambda(\lambda) \frac{c_1}{\lambda^5 (e^{c_2/\lambda T} - 1)} \cong \varepsilon_\lambda(\lambda) \frac{c_1}{\lambda^5 e^{c_2/\lambda T}}. \quad (8)$$

This yields a set of equations that are linear with respect to the inferred temperature and unknown emissivity coefficients.

In this study, the non-linear least-squares technique is used for models 2, 3 and 4, and the linear least-squares technique for the rest of the models. Note that T_λ in models 6, 7-1, 7-2, 8-1, and 8-2, is not the inferred temperature but the equivalent blackbody temperature of the measured spectral intensity.

Tables 2 and 3 provide absolute errors in the inferred temperatures for measured surface temperatures of 600 and 700 K, respectively; 800 K data are purposely excluded because of the aforementioned strong surface discoloration at this temperature. Each table includes results for AL 1100, AL 2024, AL 7075 and AL 7150 samples with polished surfaces. Three different numbers of wavelengths are tested. For each model, the required minimum number of wavelengths, N , is equal to the number of unknown coefficients in the emissivity model plus two. One and two additional

wavelengths are then tested. The results are provided for three spectral ranges: a short range of 2.05–3.43 μm , a long range of 3.50–4.72 μm , and a combined range of 2.05–4.72 μm . Data in the CO_2 and H_2O bands are excluded from the analysis. To simplify the identification of accurate models, only errors below ± 50 K are given in the tables.

The results in Tables 2 and 3 appear somewhat puzzling at first. The occurrence of the accurate measurements with errors below 10 K is quite random. Only two cases produce exact predictions, both are for AL 7075 over the range of 2.05–3.43 μm using model 7-2 at 600 K and model 8-1 at 700 K. Near exact predictions, with errors below 1 K are also achieved for a few cases, but with no clear pattern. A more systematic means for identifying useful trends regarding preferred models is therefore needed. Below is a discussion of the individual effects of spectral range, number of wavelengths, number of unknown coefficients, temperature, and alloy composition on the accuracy of different MRT emissivity models.

4.1. Effects of spectral range

Doloresco [5], Gardner [12], and Gathers [13] suggested a broader wavelength range can reduce the error in the inferred temperature. However, Tables 2 and 3 show “acceptable results” (designation used loosely here to denote temperature errors below ± 50 K) are observed not only in the combined wavelength range of 2.05–4.72 μm , but in the short wavelength range of 2.05–3.43 μm as well. This suggests broadening the wavelength range does not necessarily improve measurement accuracy. Different emissivity models appear to be more suitable over a narrower wavelength range and less successful over the broader range. This is not surprising considering the complexity of emissivity distributions shown earlier in Figs. 5 and 8.

4.2. Effects of number of wavelengths

One feature which makes MRT more accurate than SRT and DWRT is that an increase in the number of wavelengths facilitates statistical reduction of temperature errors from measurement noise. Recall that the minimum number of wavelength required in MRT is N , which is the sum of unknown coefficients, n , in the emissivity model plus two. However, Tables 2 and 3 prove, for most models, that increasing the number of wavelengths (i.e. using $N + 1$ or $N + 2$) does not enhance measurement accuracy. The required minimum number of wavelengths, N , appears to yield satisfactory results using both the linear and non-linear least-squares techniques. These findings are consistent with earlier findings by Doloresco [5], Gathers [13], and Gardner [14].

Table 2
 Absolute error in inferred temperature of polished aluminum alloy samples at 600 K

Model	N^*	Wavelength (μm)											
		2.05–3.43				3.50–4.72				2.05–4.72			
		AL 1100	AL 2024	AL 7075	AL 7150	AL 1100	AL 2024	AL 7075	AL 7150	AL 1100	AL 2024	AL 7075	AL 7150
1-1	N	6.5	20.4	45.3	–32.9								
	$N+1$												
	$N+2$	–24.9	–8.7	18.5									
1-2	N												
	$N+1$												
	$N+2$												
1-3	N												
	$N+1$												
	$N+2$												
2-1	N									–11.2	41.0	47.7	18.8
	$N+1$						14.2	16.6	13.5	–9.8			40.5
	$N+2$					–13.0	21.7	25.5	14.8	–11.5	49.3		27.6
2-2	N			–45.0									
	$N+1$												
	$N+2$			–46.9				–14.4					
2-3	N	34.2	–45.7	–30.8	–13.6			–24.7					
	$N+1$											–40.6	
	$N+2$									29.5	31.2		14.4
3	N	0.7	–8.1	–0.1	–17.6								
	$N+1$	28.5	13.2	17.7	10.7								
	$N+2$	26.3	15.6	18.8	9.5								
4	N												
	$N+1$												
	$N+2$												
5	N	–1.9	11.3	34.7	–26.1								
	$N+1$			7.9			6.4						
	$N+2$	–19.2	–9.4	11.3	–45.5				34.5				
6	N												
	$N+1$					23.8			31.1				
	$N+2$												
7-1	N												
	$N+1$												
	$N+2$												
7-2	N	–21.0	1.0	13.0	–18.7								
	$N+1$	–23.3	–21.8	–1.7	–35.1								
	$N+2$	–23.3	–13.7	0.0	–31.0								
8-1	N									22.3	26.6	30.9	18.1
	$N+1$									20.1	26.2	30.4	17.7
	$N+2$									20.2	25.5	30.0	16.4
8-2	N	5.3	27.1	42.9	2.9								
	$N+1$	9.7	8.4	36.2	–8.4								
	$N+2$	2.5	11.2	29.3	–10.3								
9-1	N		43.2	48.7	36.2					–5.2	0.5	4.6	–7.8
	$N+1$		46.1		39.3					–9.4	–1.5	2.7	–10.2
	$N+2$				44.2					–9.7	–2.1	2.4	–11.1

(continued on next page)

Table 2 (continued)

Model	N^*	Wavelength (μm)											
		2.05–3.43				3.50–4.72				2.05–4.72			
		AL 1100	AL 2024	AL 7075	AL 7150	AL 1100	AL 2024	AL 7075	AL 7150	AL 1100	AL 2024	AL 7075	AL 7150
9-2	N	-39.3	-16.7	10.6									
	$N+1$	41.3	41.3		31.0								
	$N+2$			-22.8									
10-1	N					13.4	26.9	-15.7					
	$N+1$					-16.0	-5.5	-34.3					
	$N+2$					42.2		14.7					
10-2	N												
	$N+1$								-46.4				
	$N+2$					16.5							

Missing values correspond to errors beyond $\pm 50\text{K}$.

* N is minimum number of wavelengths required in MRT model, which is equal to number of unknown coefficients in model plus two.

4.3. Effects of number of unknown coefficients

Excepting models 7-2 and 8-2 over the 2.05–3.43 μm range at 600 K, Tables 2 and 3 reveal incorporating more unknown coefficient does not enhance measurement accuracy. This is consistent with earlier findings by Coates [4].

4.4. Effects of temperature

The significant changes of emissivity spectra for aluminum alloys at different temperatures were discussed earlier in this paper. These changes are reflected in different temperature prediction trends in Tables 2 and 3 for the MRT emissivity models corresponding to 600 and 700 K, respectively. Nonetheless, some of models, such as 8-1 and 9-1, appear more successful at compensating for emissivity variations due to the temperature differences. However, it is difficult to conclude which model shows the best compensation for the temperature differences.

4.5. Effects of alloy composition

In both tables, most emissivity models appear alloy independent despite differences in the value of inferred temperature. Using the required minimum number of wavelengths and applying the appropriate spectral range, models 1-1, 2-1, 2-3, 3, 5, 7-2, 8-1, 8-2 and 9-1 show acceptable compensation for all alloys at 600 K. However, at 700 K, only 8-1 and 9-1 show acceptable compensation for the different alloys, but not AL 1100.

In summary, models 1-2, 1-3, 6, and 10-2 show the poorest overall compensation and are not recommended

for aluminum alloys. Contrastingly, models 8-1 and 9-1 provide the best overall compensation for different alloys and different temperatures.

It is important to emphasize that these findings concern only polished aluminum surfaces. Since practical aluminum surfaces possess unique surface characteristics, the present study should serve as a basis for selecting emissivity models that can tackle different surface finishes. This is a primary goal of ongoing research efforts by the present authors.

5. Conclusions

This study examined the emissivity characteristics of polished aluminum alloy surfaces. Experiments were performed to measure the emissivity characteristics for several alloys over the range of 2.05–4.72 μm , subject to variations in temperature and heating time. The experimental results are used to assess the accuracy of different MRT emissivity models at temperature measurement of aluminum surfaces. Key findings from the study are as follows:

- (1) Aluminum alloy surfaces buck the general trend of increasing emissivity with increasing temperature for metallic surfaces in the infrared range. Only AL 7150 follows the expected trend, while the emissivity of the other alloys decreases between 600 and 700 K and increases between 700 and 800 K, and the emissivity of commercially pure aluminum (AL 1100) decreases monotonically with increasing temperature. The increase in emissivity at 800 K is attributed to surface discoloration that occurs at this high temperature.

Table 3
 Absolute error in inferred temperature of polished aluminum alloy samples at 700 K

Model	N^*	Wavelength (μm)											
		2.05–3.43				3.50–4.72				2.05–4.72			
		AL 1100	AL 2024	AL 7075	AL 7150	AL 1100	AL 2024	AL 7075	AL 150	AL 1100	AL 2024	AL 7075	AL 7150
1-1	N	4.6											
	$N+1$	18.9											
	$N+2$	−48.3											
1-2	N												
	$N+1$												14.4
	$N+2$												
1-3	N												
	$N+1$												
	$N+2$												
2-1	N		−2.3		5.2	27.4							−29.2
	$N+1$				41.0	−1.5	23.6						−33.1
	$N+2$		20.5	19.7	−7.7	16.4	43.0						−39.6
2-2	N	35.5											
	$N+1$									47.4			−1.9
	$N+2$									22.6			−32.9
2-3	N	−11.6			25.1					34.6			
	$N+1$												
	$N+2$							−48.3		−2.4			
3	N	11.6											
	$N+1$	28.1	−36.7	−33.2									
	$N+2$	26.1	−40.1	−44.8									
4	N		28.2		−0.4								
	$N+1$				28.0								
	$N+2$				25.2								
5	N	3.1	−21.9										
	$N+1$	4.2						38.6					
	$N+2$	−38.7											
6	N				29.8	9.8							
	$N+1$												
	$N+2$												
7-1	N							22.0				28.1	
	$N+1$							8.6				18.9	
	$N+2$											21.9	
7-2	N	−25.1											
	$N+1$	−7.2											
	$N+2$	−24.6											
8-1	N		11.3	0.0	0.6					24.6	−27.0		−21.1
	$N+1$		21.5	15.5	6.5					22.1	−28.5		−20.5
	$N+2$		21.8	13.8	8.0					22.7	−28.3		−19.7
8-2	N	16.8											
	$N+1$	40.8											
	$N+2$	15.4								4.5			
9-1	N		−15.0	−26.5	−26.7					−6.8			−47.4
	$N+1$		−4.4	−11.0	−20.9					−11.2			−47.4
	$N+2$		−4.0	−142.4	−19.6					−10.6			−46.8

(continued on next page)

Table 3 (continued)

Model	N^*	Wavelength (μm)											
		2.05–3.43				3.50–4.72				2.05–4.72			
		AL 1100	AL 2024	AL 7075	AL 7150	AL 1100	AL 2024	AL 7075	AL 150	AL 1100	AL 2024	AL 7075	AL 7150
9-2	N $N+1$ $N+2$	-37.4											
10-1	N $N+1$ $N+2$						14.7 -5.4						
10-2	N $N+1$ $N+2$					-10.3							

Missing values correspond to errors beyond $\pm 50\text{K}$.

* N is minimum number of wavelength required in MRT model, which is equal to number of unknown coefficients in model plus two.

- (2) Surface oxidation increases the emissivity of aluminum alloy surfaces when maintained at a constant elevated temperature. However, this increase is limited to the first three hours of exposure to the elevated temperature. This suggests a strong relationship between emissivity and oxidation rate during the initial period of oxidation buildup. Thereafter, the emissivity remains constant, apparently the result of the oxidation layer becoming fully developed.
- (3) Assessment of 18 emissivity models provides important trends concerning the application of these models for aluminum temperature measurement. First, many of the models provide acceptable results in either the short wavelength range of 2.05–3.43 μm or in the combined range of 2.05–4.72 μm , but not both. This is the result of the drastic changes in the emissivity distribution precluding the use of a single function to accurately represent every band of the measured spectrum. Second, the present assessment proves increasing the number of wavelengths above that required by MRT (number of unknown coefficients in emissivity model plus two) does not enhance measurement accuracy. Thirdly, increasing the number of unknown coefficients in an emissivity model (e.g., using a higher order function) does not improve temperature predictions.
- (4) Overall, two relatively simple models, 8-1 (exponential function of $1/T_\lambda$) and 9-1 (exponential of linear first order function of $\sqrt{\lambda}$), provide the best overall compensation for different alloys and temperatures.
- (5) Despite the relative success of two of the MRT models, the present study clearly demonstrates that significant improvements are required in both

instrumentation and emissivity models to achieve acceptable accuracy in the implementation of radiation thermometry in the aluminum industry.

Acknowledgments

Financial support of the Indiana 21st Century Research and Technology Fund is gratefully appreciated. The authors also thank Mr. Gerry Dail of ALCOA for supplying aluminum samples, and Dr. Jongmook Lim of Spectraline Inc. for his technical assistance.

References

- [1] M.A. Pellerin, Multispectral radiation thermometry for industrial applications, PhD thesis, Purdue University, West Lafayette, IN, 1999.
- [2] R. Siegel, J.R. Howell, Thermal Radiation Heat Transfer, McGraw-Hill, New York, NY, 1972.
- [3] D.K. Edwards, I. Catton, Advances in the thermophysical properties at extreme temperatures and pressures, in: Proc. Symp. on Thermophysical Properties, Purdue University, West Lafayette, IN, 1965, pp. 189–199.
- [4] P.B. Coates, Multi-wavelength pyrometry, Metrologia 17 (1981) 103–109.
- [5] B.K. Doloresco, Review of multispectral radiation thermometry and development of constrained minimization method, MS thesis, Purdue University, West Lafayette, IN, 1986.
- [6] M.J. Haugh, Radiation thermometry in the aluminum industry, in: D.P. DeWitt, G.D. Nutter (Eds.), Theory and Practice of Radiation Thermometry, John Wiley, New York, NY, 1988.

- [7] M.A. Pellerin, Multispectral radiation thermometry: emissivity compensation algorithms, MS thesis, Purdue University, West Lafayette, IN, 1990.
- [8] M.A. Pellerin, D.P. DeWitt, G.J. Dail, Multispectral radiation thermometry for aluminum alloys, in: *Heat Transfer in Metals and Containerless Processing and Manufacturing*, HTD-Vol. 162, ASME, New York, NY, 1991, pp. 43–47.
- [9] M.A. Pellerin, B.K. Tsai, D.P. DeWitt, G.J. Dail, Emissivity compensation method for aluminum alloy temperature determination, in: J.F. Schooley (Ed.), *Temperature, its Measurement and Control in Science and Industry*, Vol. 6, American Institute of Physics, New York, NY, 1992, pp. 871–876.
- [10] M.F. Hopkins, Four color pyrometer for metal emissivity characterization, *SPIE-Int. Soc. Opt. Eng.* 2599 (1996) 294–301.
- [11] F.P. Incropera, D.P. DeWitt, *Fundamentals of Heat and Mass Transfer*, fourth ed., John Wiley and Sons, New York, NY, 1996, p. 657.
- [12] J.L. Gardner, Computer modeling of multiwavelength pyrometer for measuring true surface temperature, *High Temp.–High Press.* 12 (1980) 699–705.
- [13] G.R. Gathers, Analysis of multiwavelength pyrometry using nonlinear chi-square fits and Monte Carlo methods, *Int. J. Thermophys.* 13 (1992) 539–554.
- [14] J.L. Gardner, T.P. Jones, M.R. Davies, A six-wavelength radiation pyrometer, *High Temp.–High Press.* 13 (1981) 459–466.